

# Fatigue evaluation for longitudinal-to-transverse rib connection of orthotropic steel deck by using structural hot spot stress

Koichi Yokozeki<sup>1</sup> · Chitoshi Miki<sup>2</sup>

Received: 23 January 2015 / Accepted: 16 October 2015 / Published online: 17 November 2015  
© International Institute of Welding 2015

**Abstract** Orthotropic steel decks have serious fatigue problems especially on the connections between longitudinal and transverse ribs. In this paper, experimental and analytical works were conducted to evaluate the fatigue performance of connections between longitudinal U-ribs and transverse ribs with and without the slit on the transverse rib web. Finite element analyses of the specimen for all possible loading cases clarified the influence surfaces for structural hot spot stress (SHSS) working on weld toes of the connections. Fatigue tests with the loading case that generates the maximum and minimum SHSS on the connections were conducted. Fatigue test results for the slit connections evaluated by SHSS show agreement with previous fatigue data of similar connection details. No fatigue crack was initiated on the connection without the slit after 4.6 million cycles compared to fatigue failure of the slit connection at 0.7 million cycles.

**Keywords** (IIW Thesaurus) Fatigue tests · Stress · Steels · Finite element analysis

## 1 Introduction

Orthotropic steel decks (OSD) are commonly used in long span bridges or city highway bridges due to their lightweight.

---

Recommended for publication by Commission XIII - Fatigue of Welded Components and Structures

---

✉ Koichi Yokozeki  
yokozeki.4dg.kohichi@jp.nssmc.com

<sup>1</sup> Nippon Steel and Sumitomo Metal, Steel Structures Research Laboratory, Chiba, Japan

<sup>2</sup> Tokyo City University, Tokyo, Japan

However, many fatigue cracks from welded connections in OSD have been reported from several countries [1–3]. Figure 1 explains the locations of major fatigue cracks reported from metropolitan highway bridges in Japan [4]. Many cracks were initiated from slits at connections of longitudinal and transverse ribs as FD1 or DR2 in Fig. 1. In this study, a new connection detail that removes the slit is proposed.

Since tires pass on various transverse positions in actual bridges, it is important to clarify the relation of tire load locations to fatigue behavior of OSDs. In this study, the relation of tire load locations to structural hot spot stresses (SHSS) working at weld toes is investigated by finite element analysis (FEA). SHSS, which can be determined by FEA or strain measurement at actual welded connections, has been studied and confirmed to be related to fatigue life of welded connections [5].

Fatigue tests with a structural specimen are also performed to confirm the applicability of the SHSS approach to the fatigue evaluation of the longitudinal-to-transverse rib connections.

The purpose of this study is as follows:

- (1) Clarify the relation of tire load locations to SHSS working at the longitudinal-to-transverse rib connection.
- (2) Confirm the applicability of the SHSS approach to the connection of OSD.
- (3) Evaluate the fatigue life of the connections with the slit and without the slit.

## 2 Longitudinal-to-transverse rib connection

The slits on transverse rib webs are required to enable welding of the connections even though the slits generate crack

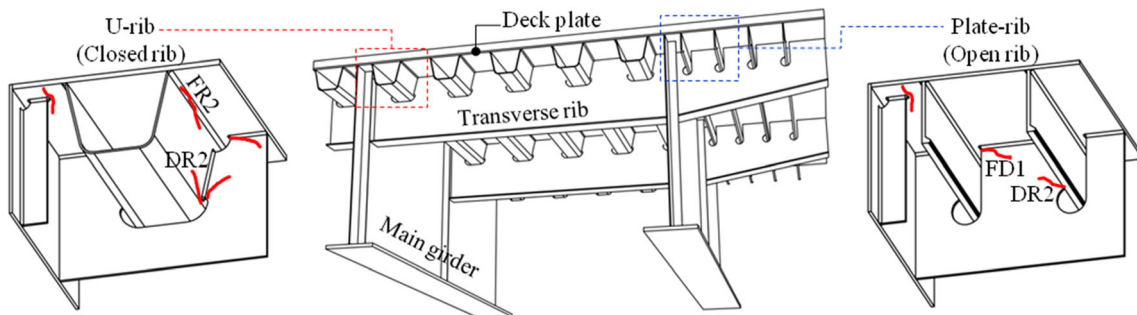


Fig. 1 Fatigue damages of OSD (red lines mean fatigue cracks)

Fig. 2 Various connection details (dimensions in millimeter)

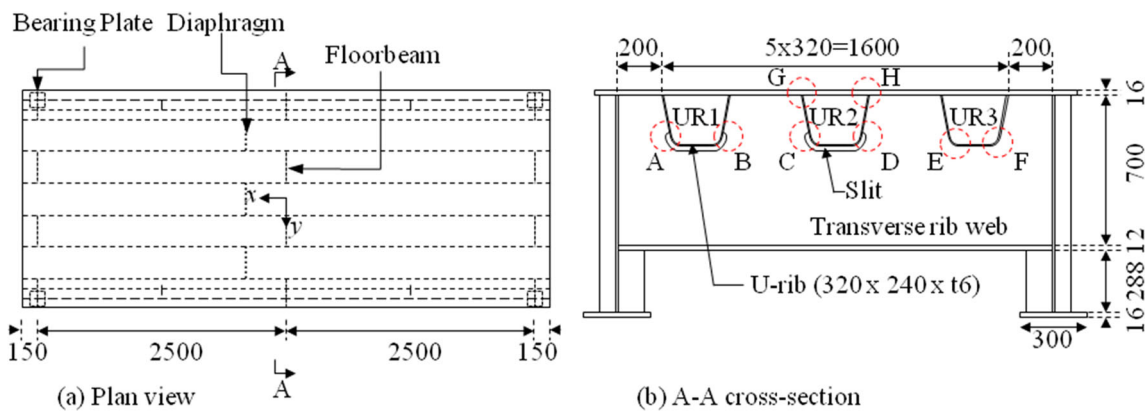
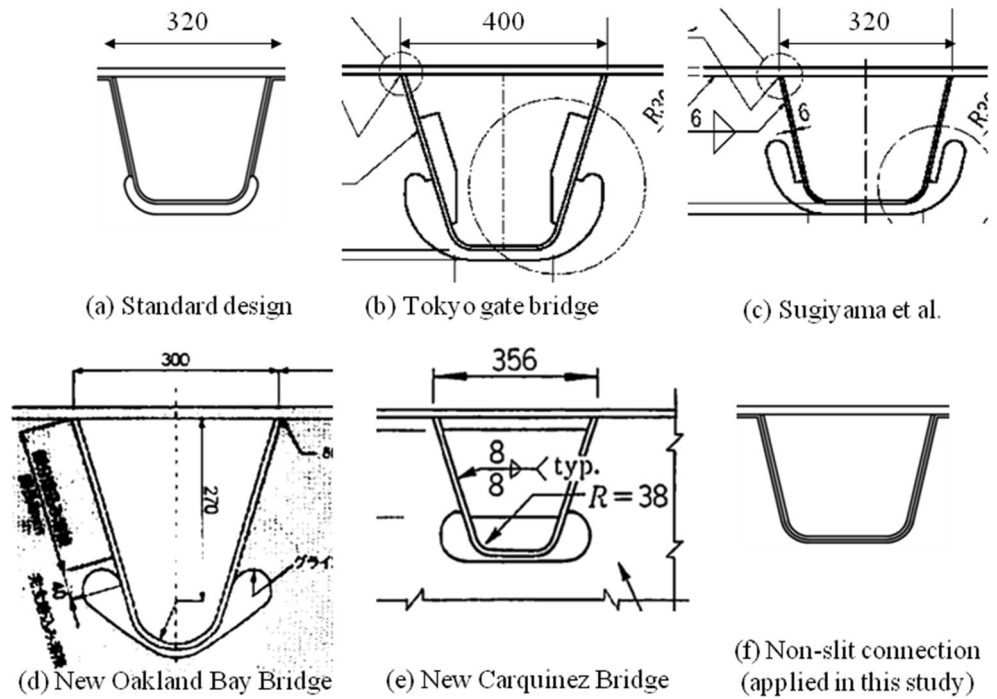
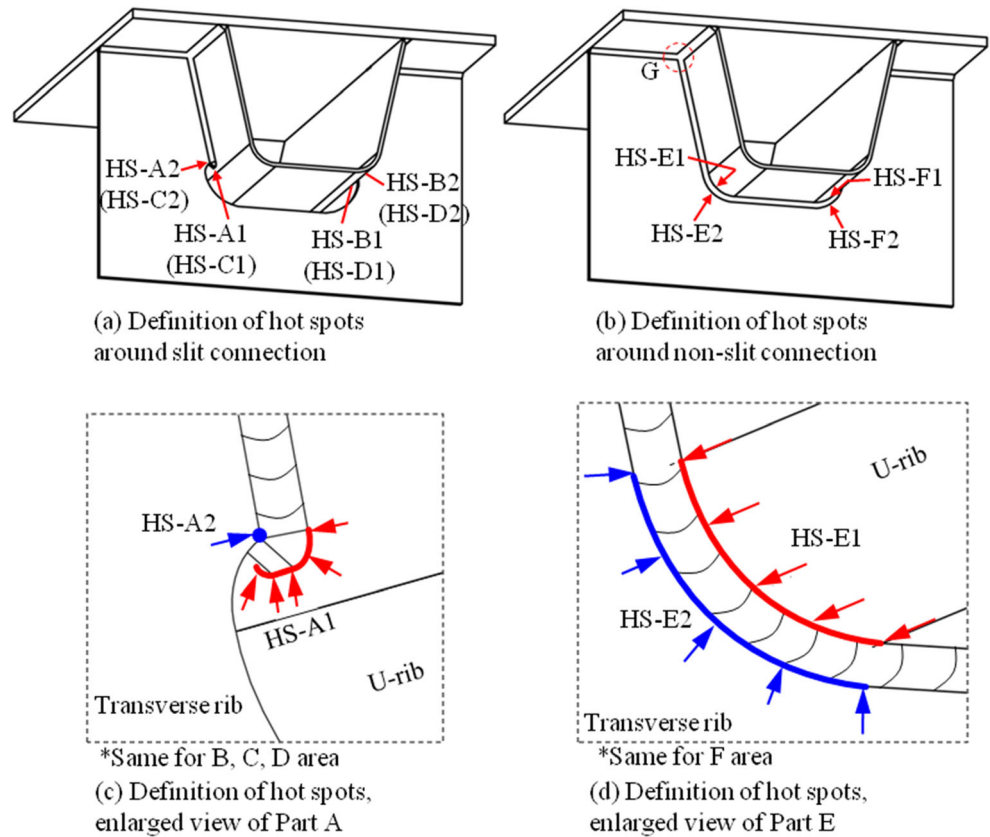


Fig. 3 Model (dimensions in millimeter)

Fig. 4 Definition of hot spots



initiation points. Previous studies have proposed the shapes of the slits or attachments to improve fatigue performance [6]. OSD of Tokyo gate bridge [7] and Hanshin highway [8], shown in Fig. 2, adopted the connection detail with the improved slit shape to reduce the stress concentration at the end of the slit. The former connection was combined with an inner rib. The New San Francisco Oakland Bay Bridge [9] adopted the longitudinal rib with the V shape cross-section. A diaphragm (bulk head) was applied to the connection of OSD in the New Carquinez Bridge [10].

In contrast, fatigue performance of the non-slit connection that removes the slit is investigated in this study. The non-slit connection can be manufactured by modifying the fabrication procedure.

### 3 Model

The specimen including three longitudinal U-ribs, three transverse ribs, and two main girders is shown in Fig. 3. Numbers of U-ribs and transverse ribs were determined for the specimen to include the area affecting the fatigue problem of the connections between U-ribs and the center transverse rib according to a previous study [11]. Dimensions of ribs are determined to be of a common

OSD design in Japan. The thickness of the deck plate is 16 mm, which is the minimum thickness for the fatigue damage at the connection of U-ribs and deck plate [12]. Mild steel (JIS-SM400) is used for the materials of all members.

The target connection is intersections of the center transverse rib and the three longitudinal U-ribs. Two of the intersections have the slits and the other does not have the slit.

Diaphragms are installed in all U-ribs of the model to create the harsh condition for the target connection. Diaphragms, which are installed for rust proofing, increase the stress value working at the connections of longitudinal-to-transverse ribs and accelerate the initiation of fatigue cracks.

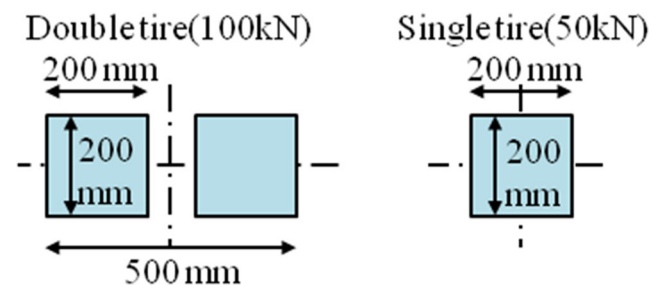


Fig. 5 Tire loads

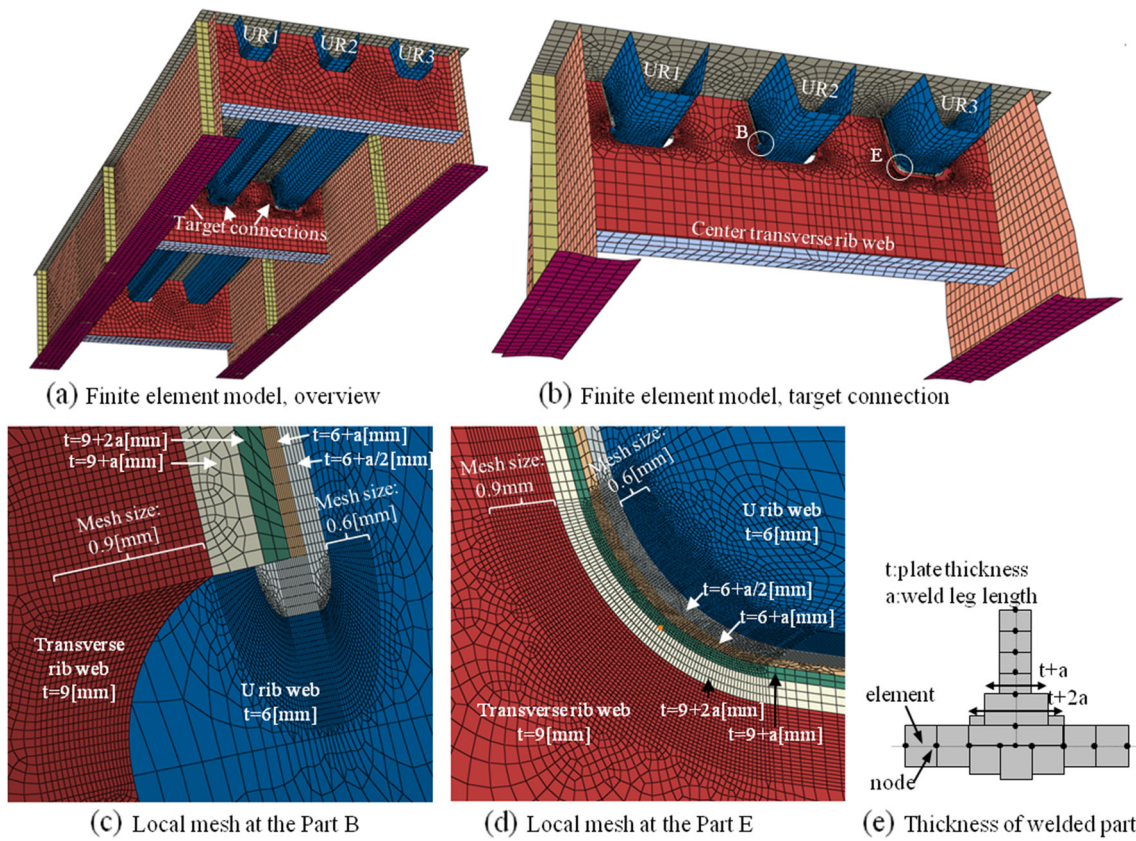


Fig. 6 Finite element model

Highly stressed parts were named A~H as indicated in Fig. 3b, where the diaphragm side surface of the center transverse rib was defined as obverse. Parts A~F have the possibility of fatigue crack initiation from the weld toe. The weld toes (hot spots) were defined as illustrated in Fig. 4. In contrast, weld root cracks may be initiated from parts G and H.

The track tire load shown in Fig. 5 is modeled according to the specifications for highway bridges in Japan [13]. The specimen is supported at the bearing plates attached under the lower flanges of the main girders.

#### 4 Finite element analysis

Elastic finite element analyses were conducted using Abaqus 6.13 to search for the harshest condition for fatigue of the target connections. The model displayed in Fig. 6 was created with 4-node shell elements. The element sizes around the target weld toes are approximately 0.1 t. In order to consider the increased stiffness, thicknesses of shell elements at welded connections are increased as shown in Fig. 6c, d, e by reference to Niemi et al. [14].

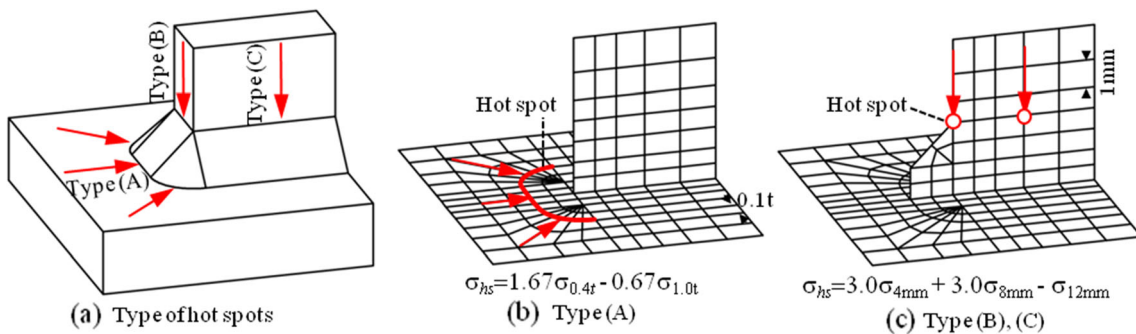


Fig. 7 Hot spot stress calculation

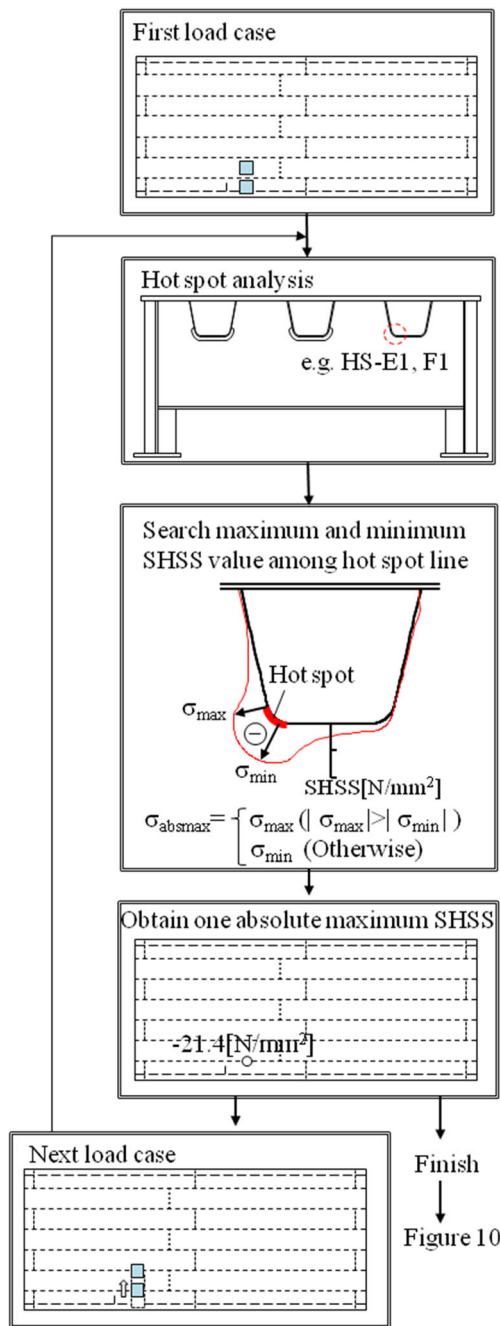


Fig. 8 Procedure of finite element analysis

SHSS at the weld toes was calculated according to the stress linearization approach provided in the IIW recommendations [15] as shown in Fig. 7. Two finite element models with different-shaped weld toes were created for two types of hot spot as illustrated in Fig. 7a.

The procedure of finite element analysis is illustrated in Fig. 8. SHSS was calculated by moving the location of the tire load by 160 and 200 mm intervals in longitudinal and transverse directions. In each load case, absolute maximum SHSS of all hot spots was calculated. Absolute maximum SHSS was determined by the following criteria where  $\sigma_{max}$  and  $\sigma_{min}$  mean the maximum and the minimum value among the distribution of SHSS around the target weld toe.

$$\sigma_{absmax} = \begin{cases} \sigma_{max} (|\sigma_{max}| > |\sigma_{min}|) \\ \sigma_{min} (Otherwise) \end{cases}$$

Figure 9 shows the distribution of SHSS at HS-B1 in the case of the load location which causes maximum stress at the weld toe. The absolute maximum value of the SHSS distribution among the weld toe, which is 311 N/mm<sup>2</sup>, was referenced as the representative SHSS value of the weld toe in the case of Fig. 9. The figure shows the membrane and bending component separately, which mean the average and half of the difference of surface stresses on both sides, respectively. Figure 9 indicates that bending stress is dominant at the HS-B1. Similar tendencies were found in all U-rib side weld toes of the slit connection. According to the JSSC fatigue recommendations [16], fatigue strength of welded joints under bending stress is 1.5 times larger than that under membrane stress. Lotsberg and Sigurdsson [17] propose reducing the bending component of the structural stress by a factor of 0.6. This paper considers both the normal SHSS and the SHSS considering bending stress reduction according to the JSSC fatigue recommendation. The following equation shows the latter SHSS.

$$\sigma'_{hs} = \sigma_{hs,m} + \frac{\sigma_{hs,b}}{1.5} \tag{1}$$

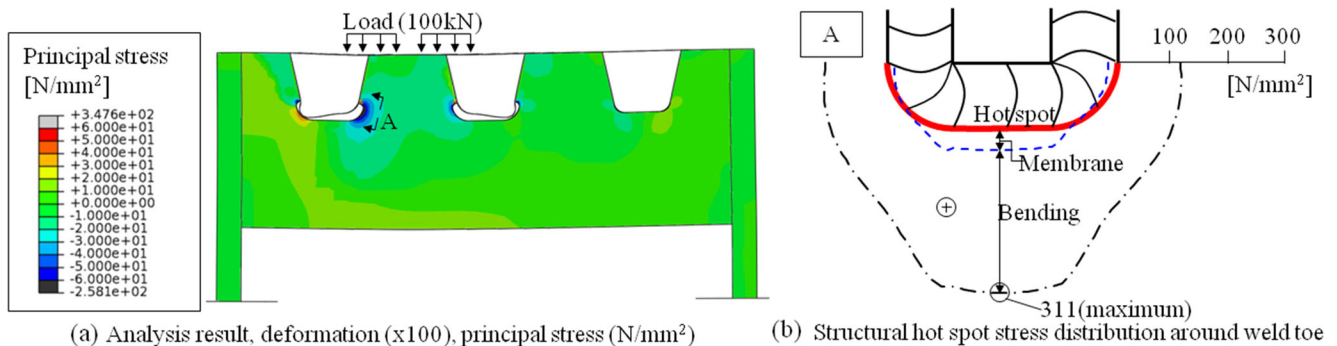


Fig. 9 FEA result, SHSS distribution at HS-B1

Fig. 10 Influence surface

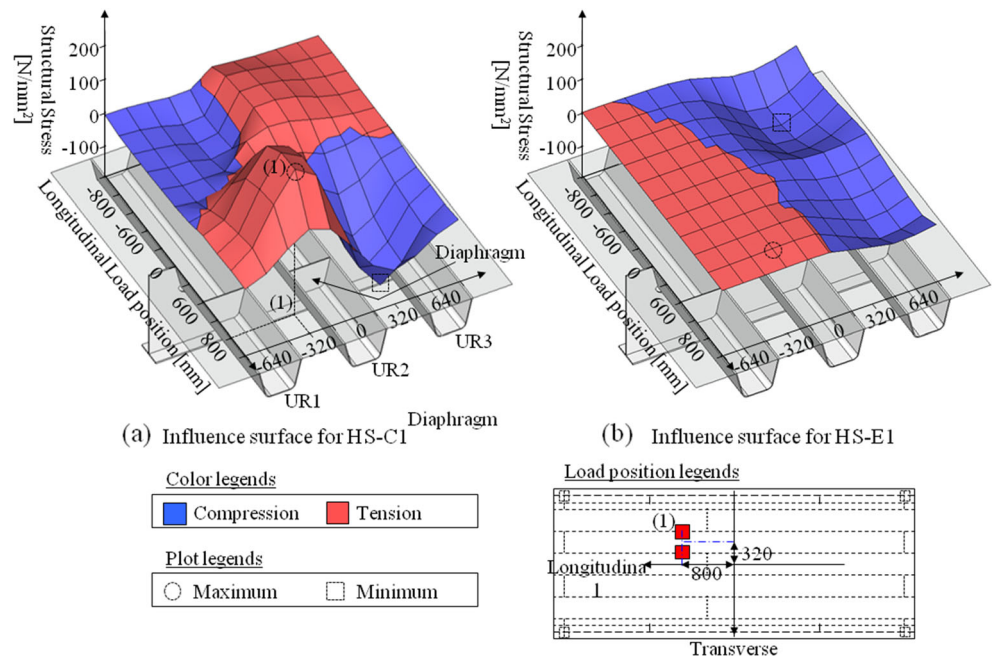


Fig. 11 Maximum and minimum SHSS

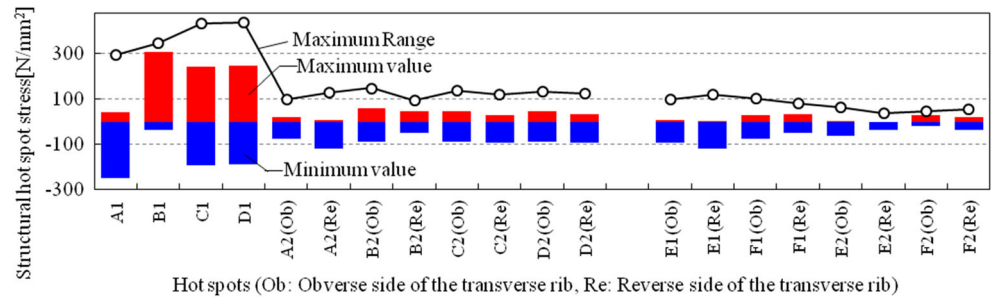


Fig. 12 Fatigue test setting

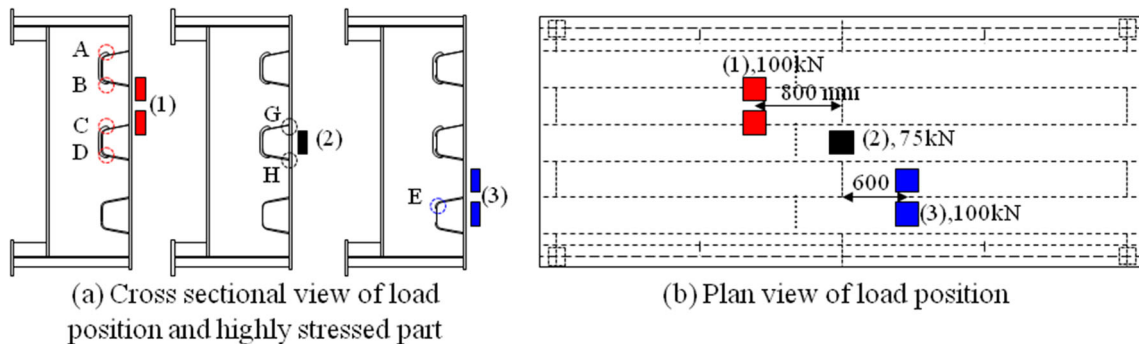
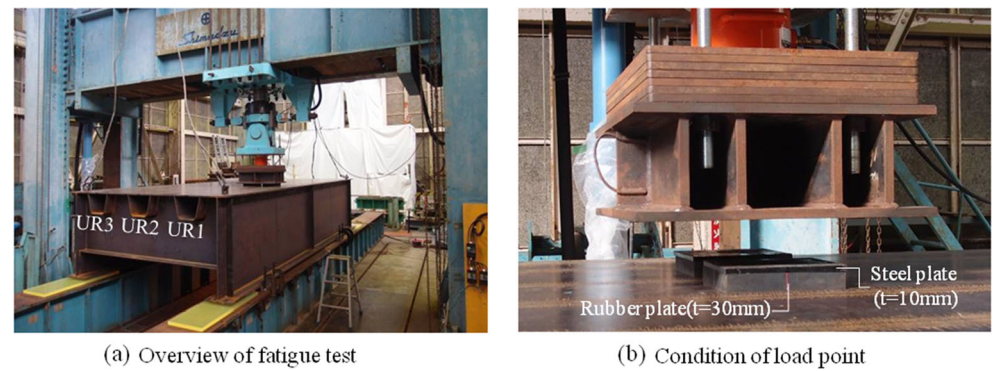


Fig. 13 Load case for fatigue test

where  $\sigma_{hs,m}$  and  $\sigma_{hs,b}$  mean membrane and bending components of SHSS.

The influence surfaces for each hot spot displayed in Fig. 10 show the relation of tire load locations to absolute maximum SHSS. The influence surface includes two details: the maximum SHSS range that affects the fatigue strength of the connection and the tire load location that causes maximum and minimum SHSS. Loading conditions for the fatigue test can be determined from the influence surface.

Fatigue evaluation for OSDs in actual structures requires the influence surface or equivalent procedures because SHSS of longitudinal-to-transverse rib connections varies depending on the longitudinal and transverse location of the tire load. It is

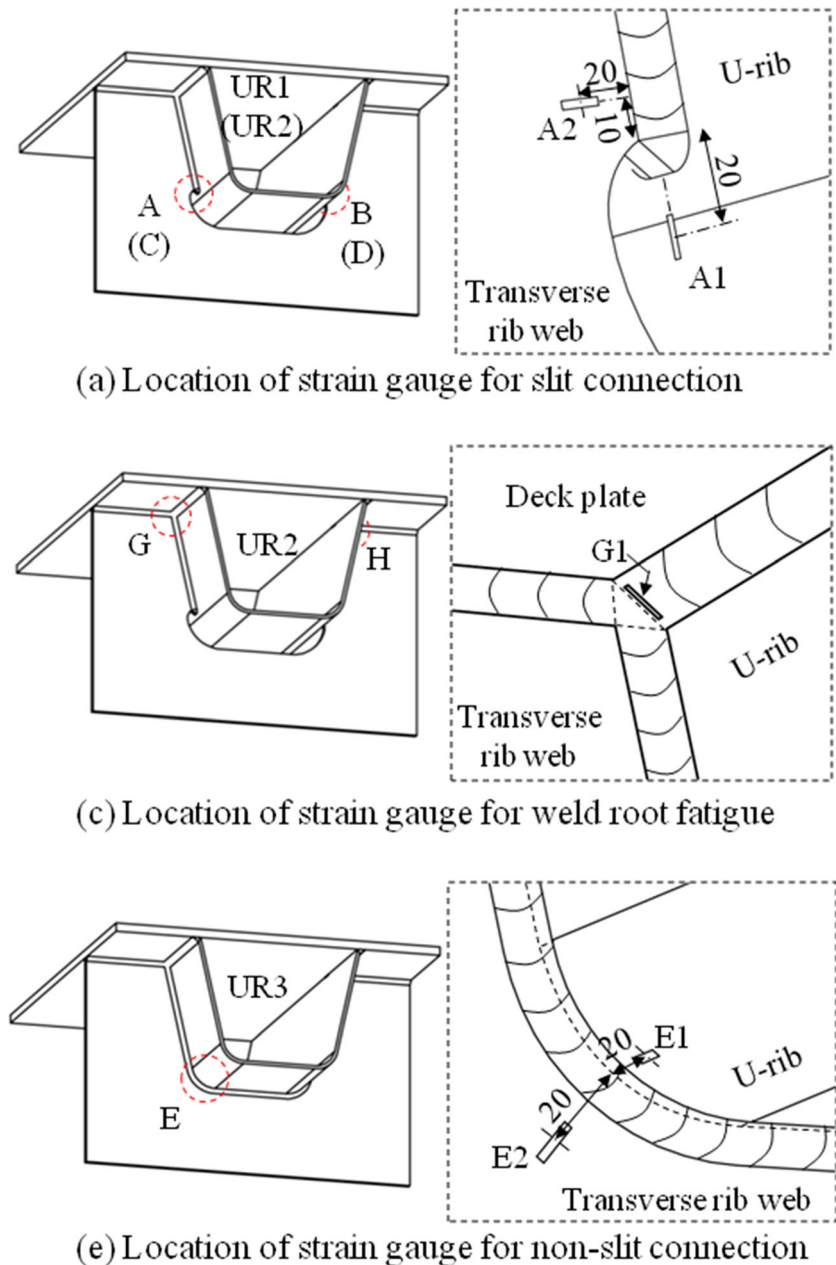
difficult to obtain a possible harshest condition without the influence surface.

The maximum and the minimum values of the influence surfaces are summarized in Fig. 11. Since HS-B1 and HS-E1 were the most stressed hot spots for the slit connection and the non-slit connection, those two hot spots were selected as the target connection of the fatigue test.

### 5 Fatigue test

The fatigue tests were conducted with constant amplitude loading (20–120 kN) as shown in Fig. 12. The load was

**Fig. 14** Arrangement of strain gauges



transferred from the 500 kN hydraulic jack to the specimen by rubber plate to simulate the actual tire load condition.

The load locations for fatigue tests, shown in Fig. 13, were determined to create the harshest conditions for the slit connection and the non-slit connection, which are load locations that generate maximum SHSS for HS-B1 (load case 1) and minimum SHSS for HS-E1 (load case 3). In addition, the fatigue test for the weld root of the connection of the longitudinal U-rib to deck plate was performed (load case 2). Fatigue tests with three load cases were performed in order of load case 1, 2, and 3 with 3.0 million, 3.0 million, and 4.6 million cycles.

In order to compare stresses of the specimen and the analysis model and to detect the initiation of fatigue crack, strains near the suspected crack initiation point were measured before and during cyclic loadings. Locations of strain gauges are indicated in Fig. 14. All strain gauges except A1, B1, C1, and D1 are attached to both sides of the center transverse rib. Strain gauge G1 and H1 were attached to the surface of the weld bead.

Measured and analyzed principal stresses were shown in Fig. 15. Measured stresses were calculated from strain with an elastic modulus of 205 kN/mm<sup>2</sup>. The largest differences of analyzed to measured principal stresses were -20 %, which was caused at HS-C2. Differences between analyzed and measured stress directions were lower than 2° in Fig. 15.

Measured strain data are shown in Fig. 16 with the vertical axis indicating the ratio of strain range to initial strain range. The strain data of B1 and C1, which were measured at the slit connection, were dropped immediately after the

start of load case 1 by the effect of crack initiation. At 0.70 million cycles, a 33-mm surface crack initiated from HS-B1 and 24-mm HS-C1 shown in Fig. 17 were detected. Those cracks, which were initiated from the weld toe and were already propagated to base material at 0.70 million cycles, were defined as fatigue failure in this study. The cracks from HS-B1 were propagated to a length of 22 mm in base material at 3.0 million cycles.

During load case 2, the fatigue cracks initiated from the weld roots caused strain drops. However, the speeds of the strain drops were slowed as crack propagated in the deck plate. The fatigue test with load case 2 was finished at 3.0 million cycles without surface crack detection. The cracks remaining in the deck plate were detected with ultrasonic testing after the fatigue test.

During load case 3 that targets the non-slit connection, strains measured around the non-slit connection were not changed. The cyclic loading was finished at 4.6 million cycles without crack initiation.

## 6 Result and discussion

According to Fig. 11, the longitudinal-to-transverse rib connection without the slit on the transverse rib web decreases the SHSS range to 120 N/mm<sup>2</sup> from 440. The stress reduction of 320 N/mm<sup>2</sup> corresponds to fatigue life improvement of 50 times, in the case that the slope of S-N diagram is 3. Since the stress range of 440 N/mm<sup>2</sup> in the non-slit connection seems to have high value, it is considered to be one of the reasons of serious fatigue problem of orthotropic steel decks.

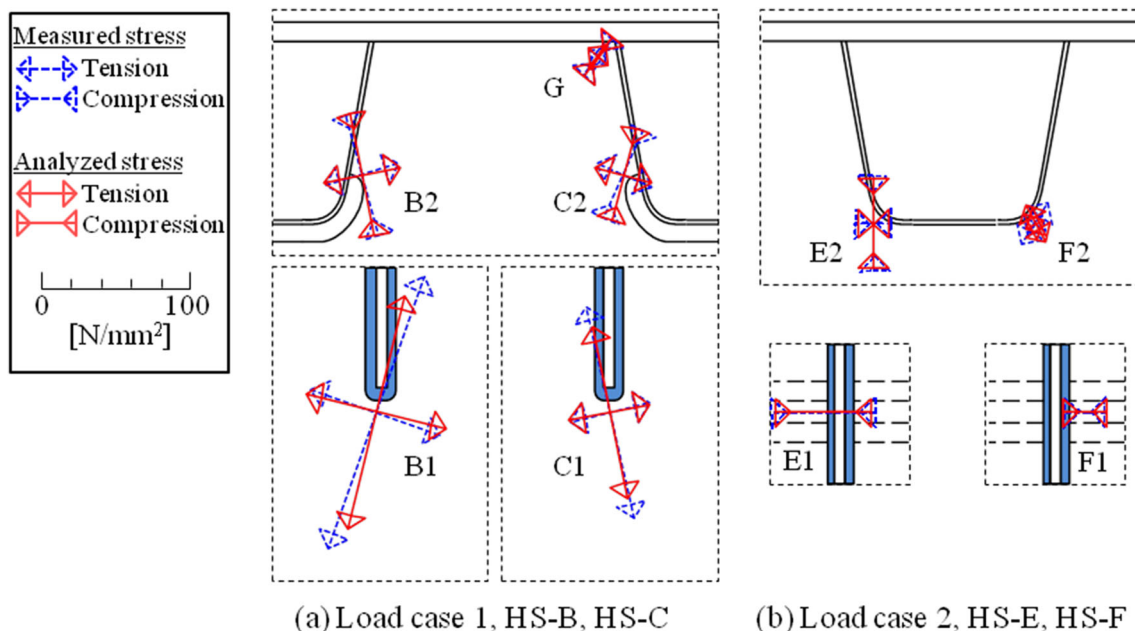


Fig. 15 Measured and analyzed principal stresses



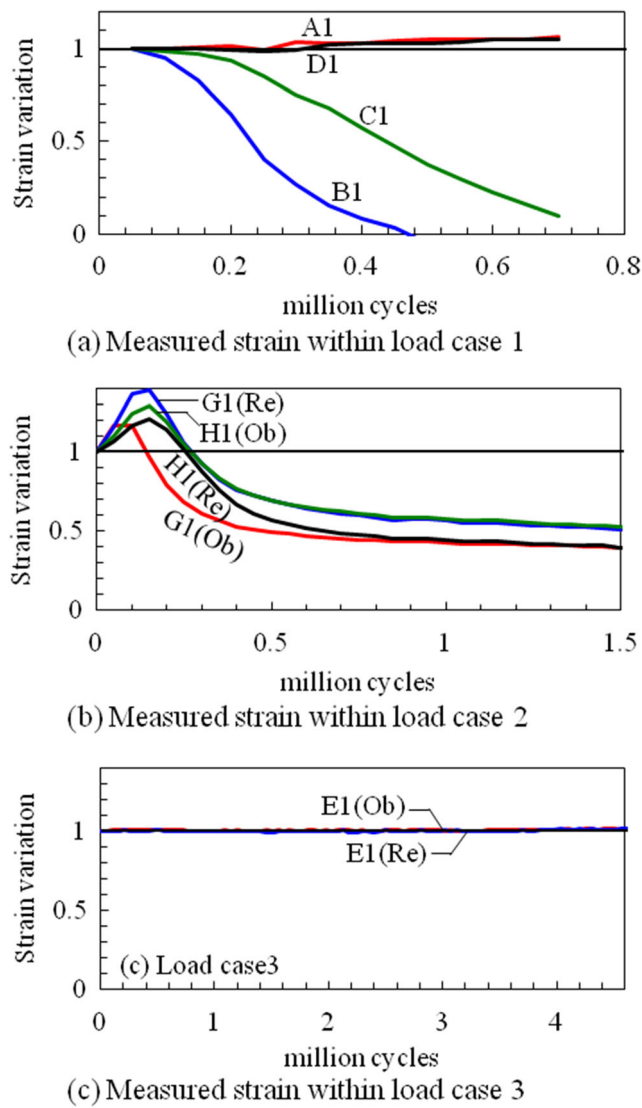
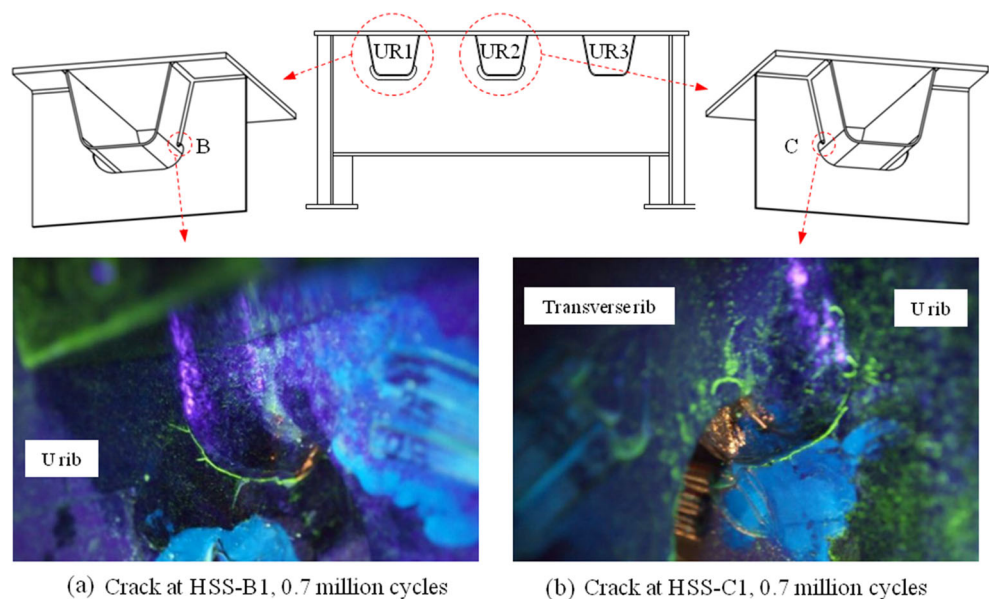


Fig. 16 Measured strains during cyclic loadings

Fig. 17 Detected fatigue crack, load case 1



The relation of the SHSS with fatigue test result shown in Fig. 18 was plotted on the safe side of FAT90 or FAT100 even though reduction of the bending stress component by Eq. (1) is considered. The results indicate that the fatigue life of longitudinal-to-transverse rib connections can be evaluated by SHSS through considering bending stress reduction even though additional fatigue data are required to design the orthotropic steel deck with SHSS.

Figure 18 includes previous fatigue data for plate specimen and structural specimen [18]. In the case of no reduction for bending stress component, the plot of the HS-A1 is located outside the upper 96 % line of the previous fatigue data. The stress condition of HS-A1, D1, and E1, where only compression stress was generated, may affect the result of the fatigue test.

### 7 Conclusion

The influence surfaces for the hot spot structural stresses (SHSSs) at the longitudinal-to-transverse rib connections with and without the slits on the transverse rib webs were calculated by elastic finite element analyses. The fatigue tests were performed with the load cases determined from the analysis result. From the analyses and experiment, the following conclusions are drawn.

- (1) SHSSs working at the longitudinal-to-transverse rib connections vary depending on the tire load location and the existence of the diaphragm as shown in Fig. 10.
- (2) Fatigue data of the longitudinal-to-transverse rib connection of OSD can be evaluated by the SHSS approach with reduction of the bending stress component.

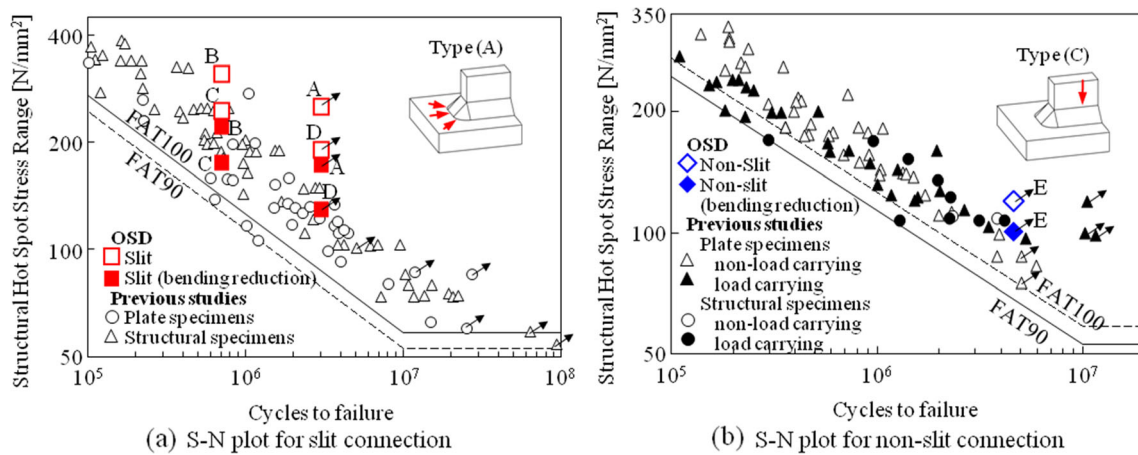


Fig. 18 Fatigue test result

- (3) The longitudinal-to-transverse rib connection without the slit on the transverse rib web decreases the SHSS range to 120 N/mm<sup>2</sup> from 440 N/mm<sup>2</sup>.

**Acknowledgments** This work was supported by the research project collaborated by following members: IHI Infrastructure Systems Co., Ltd., JFE Engineering Corporation, JFE Steel Corporation, KAWADA INDUSTRIES, INC., Kobe Steel, Ltd., KOMAIHALTEC Inc., Mitsui Zosen Steel Structures Engineering Co., Ltd., MIYAJI ENGINEERING CO., LTD., MM BRIDGE CO., LTD, NIPPON STEEL & SUMITOMO METAL CORPORATION, Yokogawa Bridge Holdings Corp.

## References

1. Wolchuk R (1990) Lessons from weld cracks in orthotropic decks on three European bridges. *J Struct Eng* 116(1):75–84
2. Subcommittee on Fatigue of Steel Orthotropic Deck (1989) Fatigue of orthotropic steel bridge deck. *J JSCE* (410):25–36
3. de Jong FBP (2004) Overview fatigue phenomenon in orthotropic steel deck in Netherland. *Proceedings of Orthotropic Bridge Conference*, Sacramento, p 489–512
4. Kinomoto T, Kajihara M, Hirabayashi Y, Konishi T, Murano M, Saito G (2008) Inspection and Retrofitting of Fatigue Damaged Orthotropic Steel Deck. *IABSE Congress Rep* 17(3):456–457
5. Radaj D, Soncino CM, Fricke W (2006) Fatigue assessment of welded joints by local approaches, 2nd edn. Woodhead publishing in materials
6. Chen W-F, Duan L (2014) *Bridge Engineering Handbook*, Second Edition: Construction and Maintenance, CRC Press
7. Morinaga M, Isogami T, Chiba T (2008) Developed technologies and achieved cost reduction through the project of Tokyo-Port Seaside Bridge (no. 3) Design of the superstructure (2), Bridges and foundation engineering 42(10):40–45
8. Sugiyama H, Tabata A, Kasugai T, Ishi H, Inokuchi S, Kiyokawa S, Ikezue K (2014) Improving fatigue resistance of cutout on diaphragm in orthotropic steel deck. *J JSCE* 70(1):18–30, **Ser. A1**
9. Chou CC, Uang CM, Seible F (2006) Experimental evaluation of compressive behavior of orthotropic steel plates for the new San Francisco-Oakland Bay Bridge. *J Bridg Eng* 11(2):140–150
10. Serzan K, Khazem D (2004) Steel orthotropic box girder on the New Alfred Zampa suspension bridge across the Carquinez Strait First in the US. *Proceeding of the 2004 Orthotropic Bridge Conference*, p 177–188
11. Miki C, Suganuma H, Tomizawa M, Machida F (2005) Cause study on fatigue damage in orthotropic steel bridge deck. *J JSCE* 2005(780 I-70):780\_57–780\_69
12. Sukanum H, Miki C (2007) Fatigue strength evaluation with effective notch stress of the weld between trough rib and deck plate on orthotropic steel deck. *J JSCE Ser A* 63(1):35–42
13. Japan Road Association (2002) *Specifications For Highway Bridges part2 steel bridge*, Maruzen
14. Niemi E (1995) Stress determination for Fatigue Analysis of Welded Components, IIW doc. IIS/IIW-1221-93
15. Hobbacher AF (2006) Recommendations for fatigue design of welded joints and components (update). IIW doc. XIII-1965-03/XV-1127-03; revision 2006
16. Japanese Society of Steel Construction (1993) *Fatigue design recommendation for steel structure*, Gihodo shuppan
17. Lotsberg I, Sigurdsson G (2006) Hot spot stress S-N curve for fatigue analysis of plated structures. *J Offshore Mech Arct Eng* 128:330–336
18. Maddox SJ (2001) Recommended hot-spot stress design S-N curves for fatigue assessment of FPSOs. *Proc Intl Offshore Polar Eng Conf* 4:97–104